

Supporting Information

Enhancement of the thermoelectric performances of bulk SnTe alloys via Synergistic effect of band structure modification and chemical bond softening

Hongchao Wang^{a,d}, Junphil Hwang^b, Chao Zhang^c, Teng Wang^a, Wenbin Su^a, Hoon
Kim^b, Jungwon Kim^b, Jinze Zhai^a, Xue Wang^a, Hwanjoo Park^b, Woochul Kim^{b*},
Chunlei Wang^{a#}

a. School of Physics, State Key Laboratory of Crystal Materials, Shandong
University, Jinan, China

b. School of Mechanical Engineering, Yonsei University, Seoul, Korea

c. School of Opto-electronic Information Science and Technology, Yantai
University, Yantai, China

d. State Key Laboratory of Metastable Materials Science and Technology, Yanshan
University, Qinhuangdao, China

* Corresponding author
E-mail address: woochul@yonsei.ac.kr (W. Kim)

Corresponding author
E-mail address: wangcl@sdu.edu.cn (C. Wang)

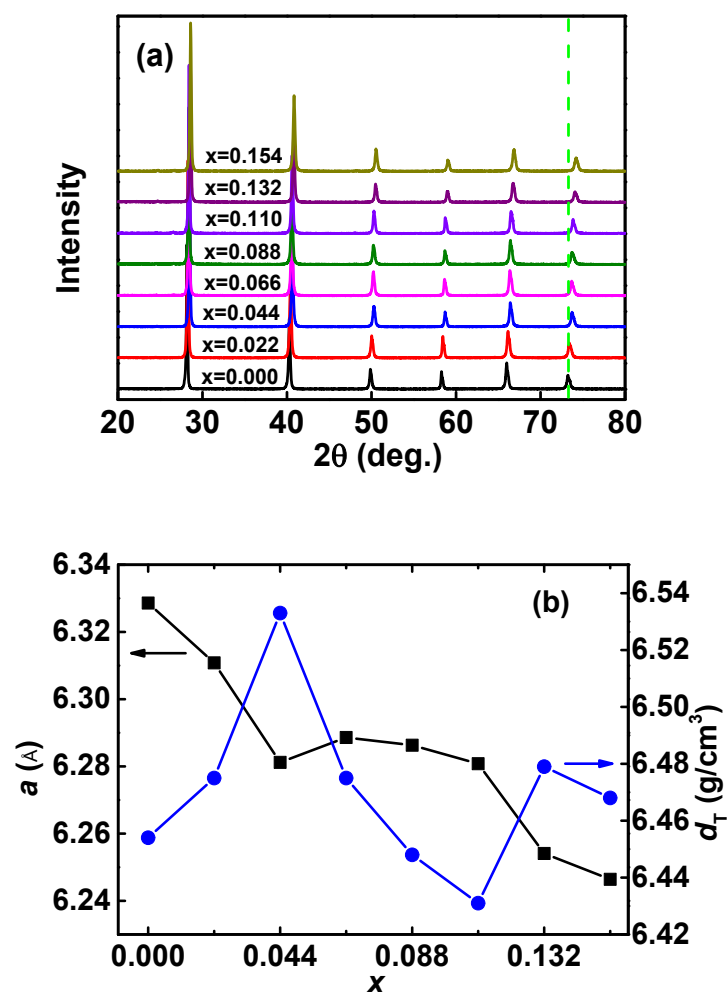


Figure S1. (a) The powder X-ray diffraction patterns of $\text{Sn}_{1-x}(\text{In}_x\text{Mn}_{10x})_{1/11}\text{Te}$ samples.

(b) Lattice constants, a , and theoretical densities, d_T , of samples as a function of doping concentration x .

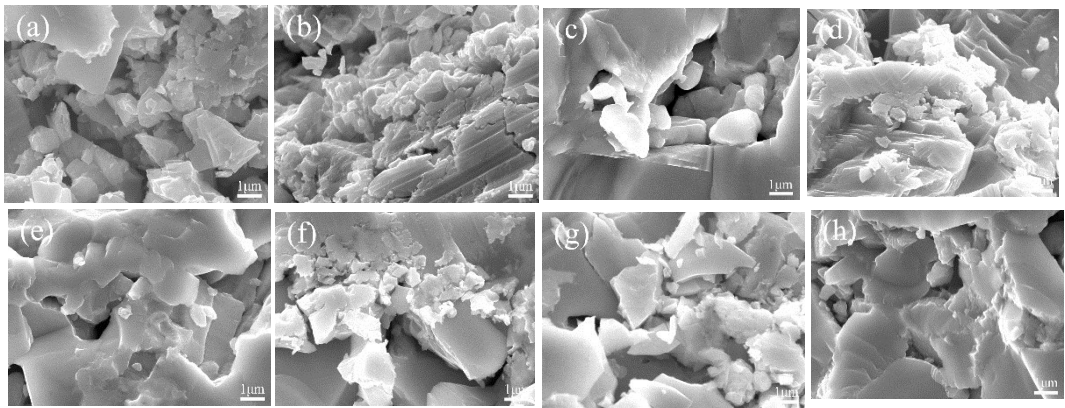


Figure S2. The cross-sectional SEM images of $\text{Sn}_{1-x}(\text{In}_x\text{Mn}_{10x})_{1/11}\text{Te}$ samples for **(a)** $x=0.000$, **(b)** $x=0.022$, **(c)** $x=0.044$, **(d)** $x=0.066$, **(e)** $x=0.088$, **(f)** $x=0.110$, **(g)** $x=0.132$, and **(h)** $x=0.154$.

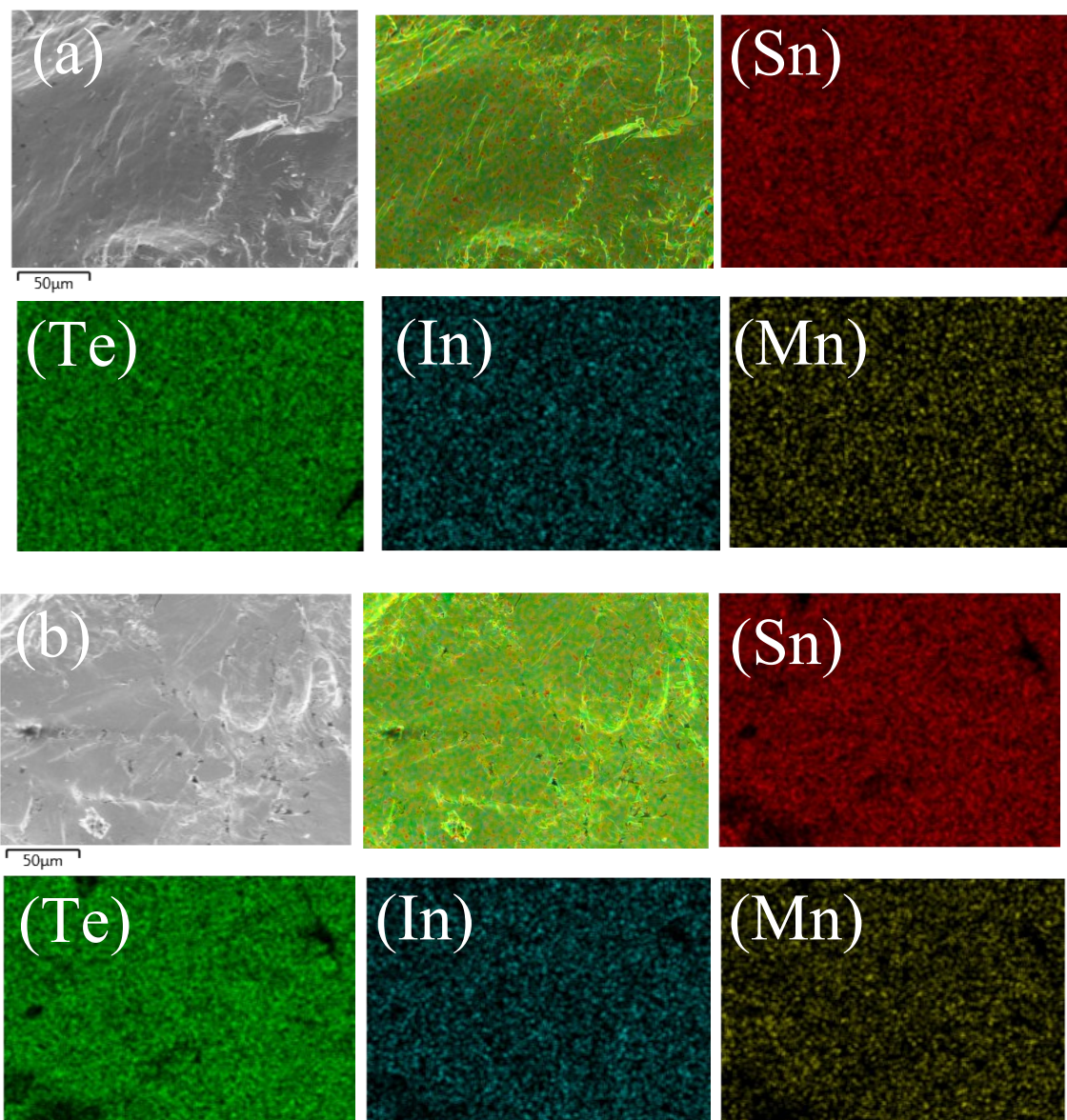


Figure S3. The SEM images with low magnification and EDS mapping for (a) $\text{Sn}_{0.89}\text{In}_{0.01}\text{Mn}_{0.1}\text{Te}$ alloy and (b) $\text{Sn}_{0.846}\text{In}_{0.014}\text{Mn}_{0.14}\text{Te}$ alloy

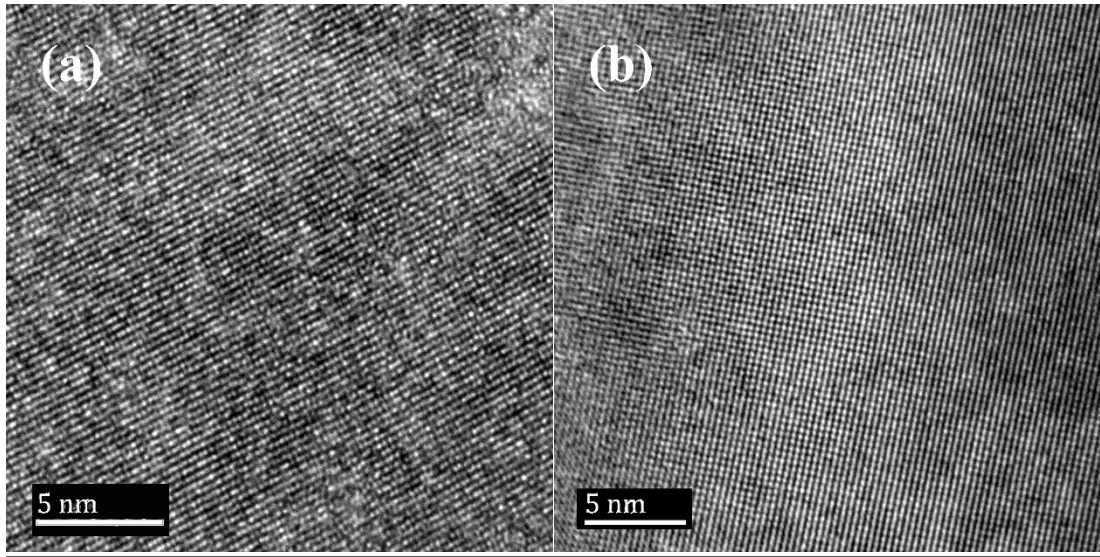


Figure S4. The TEM images for $\text{Sn}_{1-x}(\text{In}_x\text{Mn}_{10x})_{1/11}\text{Te}$ samples for (a) $x=0.000$, (b) $x=0.110$. Which are characterized by JEOL-2100F. The TEM samples are prepared by focused ion beam (FIB). In the TEM image, we cannot find nanostructures, defects and dislocations, etc, although we cannot rule out the possibility of existing these in our materials.

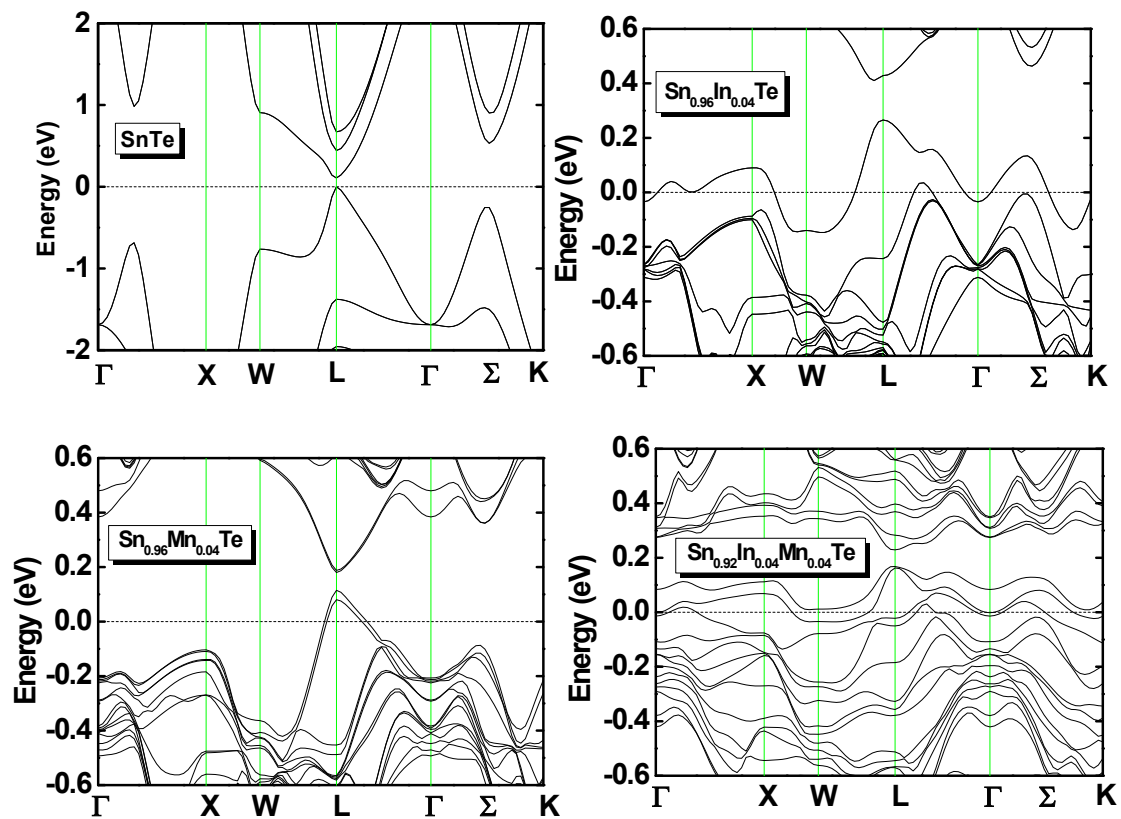


Figure S5. The electronic band structure for SnTe, $\text{Sn}_{0.96}\text{In}_{0.04}\text{Te}$, $\text{Sn}_{0.96}\text{Mn}_{0.04}\text{Te}$,

$\text{Sn}_{0.92}\text{In}_{0.04}\text{Mn}_{0.04}\text{Te}$.

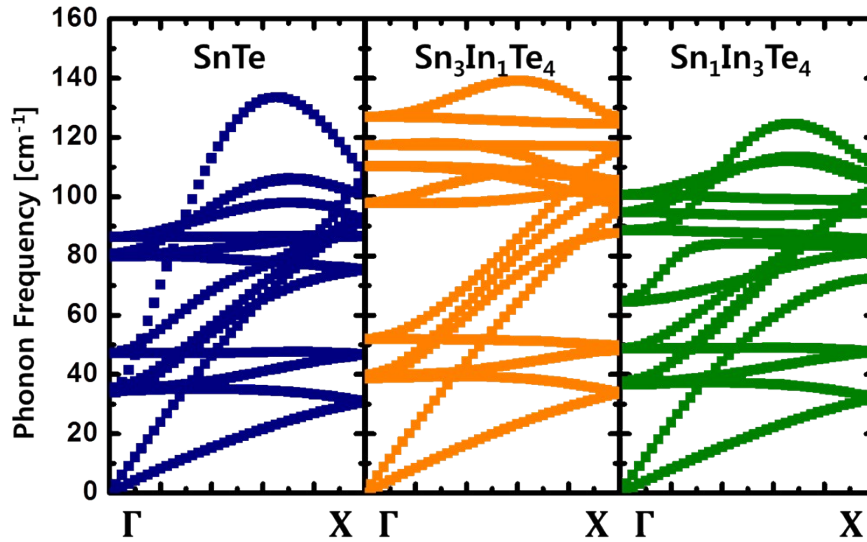


Figure S6. The phonon dispersion relation of SnTe, Sn₃In₁Te₄, Sn₁In₃Te₄ calculated composition along Γ to X. These have been done by the Quantum Espresso. Perdew-Zunger norm-conservative pseudopotentials for Sn, Te and In were used with 8 x 8 x 8 k-points Brillouin zone sampling. The kinetic energy cutoff of 60 Ry was applied. 4 x 4 x 4 q-points mesh was then applied for all phonon frequency evaluation.

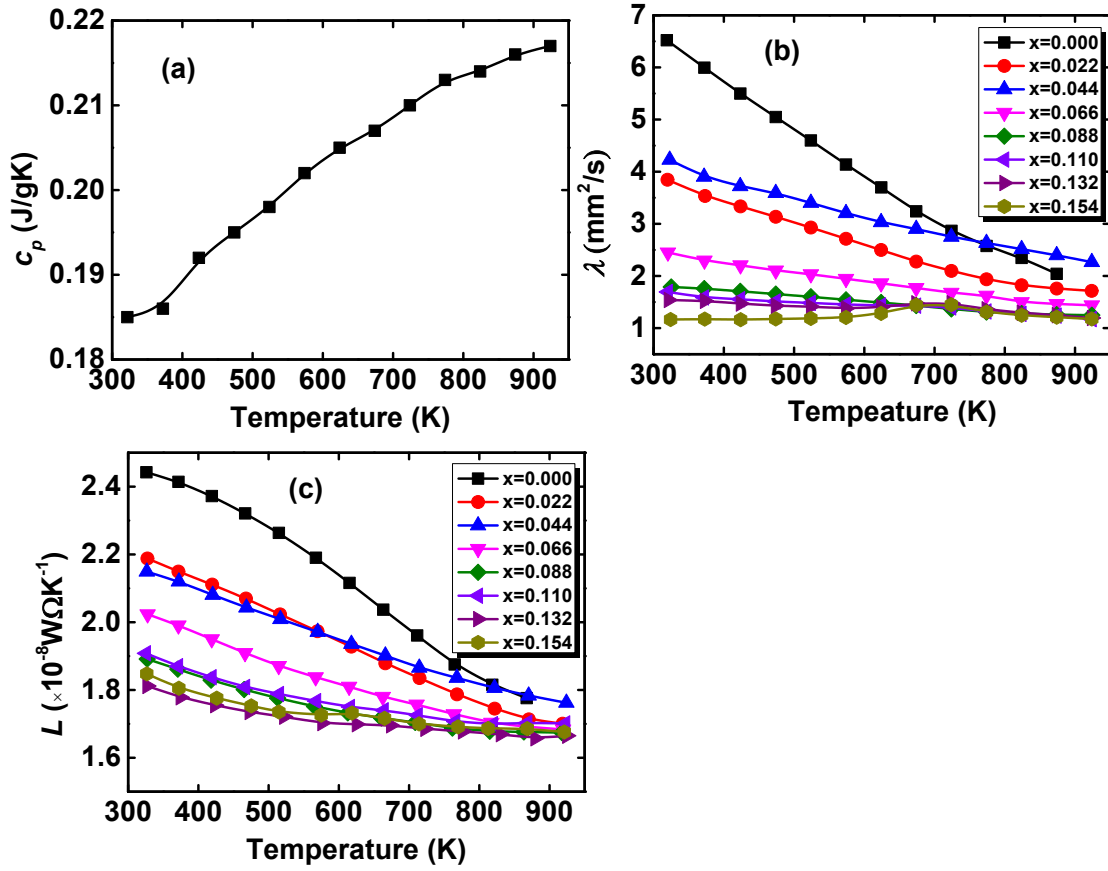


Figure S7. (a) The average heat capacity, C_p , of each sample, their values are derived using standard samples (pyroceram) in LFA457. (b) Thermal diffusivity, λ , for all samples. (c) The Lorenz number, L , for all samples derived from the equation of $L=1.5+\exp(-|S|/116)$.

Samples	d_E (g/cm ³)	Samples	d_E (g/cm ³)
x=0.000	6.19	x=0.088	6.09
x=0.022	6.13	x=0.110	6.07
x=0.044	6.14	x=0.132	6.07
x=0.066	6.10	x=0.154	6.09

Table S1. The experimental densities, d_E , for all samples.